A DISCRETE WAVELET ANALYSIS OF FREAK WAVES IN THE OCEAN

EN-BING LIN AND PAUL C. LIU

A freak wave is a wave of very considerable height, ahead of which there is a deep trough. A case study examines some basic properties developed by performing wavelet analysis on a freak wave. We demonstrate several applications of wavelets and discrete and continuous wavelet transforms on the study of a freak wave. A modeling setting for freak waves will also be mentioned.

1. Introduction

In the past few years, wavelet methods have been applied in coastal and ocean current data analysis [2, 5, 6]. These new tools have better performance than the traditional Fourier techniques. They localize the information in the time-frequency space and are capable of trading one type of resolution for the other, which renders them suitable for the analysis of nonstationary signals. It was first introduced in [5, 6] that the wavelet transform is a powerful tool for coastal and ocean engineering studies. An analysis of applying continuous wavelet transform spectrum analysis to the result of laboratory measurement of landslide-generated impulse waves was presented in [2]. In fact, the measured results are understandably unsteady, nonlinear, and nonstationary, hence the application of time-localized wavelet transform analysis is shown to be a suitable as well as a useful approach. The analysis of correlating the time-frequency wavelet spectrum configurations in connection with the ambient parameters that drive the impulse wave process, with respect to time and space, leads to interesting and stimulating insights not previously known. In [7], an analysis of a set of available freak wave measurements gathered from several periods of continuous wave recordings made in the Sea of Japan during 1986–1990 by the Ship Research Institute of Japan was presented. The analysis provides an ideal opportunity to catch a glimpse of the incidence of freak waves. The results show that a well-defined freak wave can be readily identified from the wavelet spectrum, where strong energy density in the spectrum is instantly surged and seemingly carried over to the high-frequency components at the instant the freak wave occurs. Thus for a given freak wave, there appears a clear corresponding signature shown in the time-frequency wavelet spectrum.

In fact, there is a considerable interest in understanding the occurrence of freak waves. There are a number of reasons why freak wave phenomena may occur. Often, extreme wave events can be explained by the presence of ocean currents or bottom topography that may cause wave energy to focus on a small area because of refraction, reflection, and wave trapping [3]. In this paper, we study wavelet analysis for a given time series, namely, we examine various wavelet tools on a given signal. We present several different aspects of wavelet analysis, for example, wavelet decomposition, discrete and continuous wavelet transforms, denoising, and compression, for a given signal. A case study examines some interesting properties developed by performing wavelet analysis in greater detail. We present a demonstration of the application of wavelets and wavelet transforms on waves. Here we use Daubechies wavelet (db3) in most of our applications unless otherwise specified in the context.

2. Wavelet transform

2.1. 1D continuous wavelet transforms. First, we review the standard continuous wavelet transforms. The continuous wavelet transform of a function $f(x) \in L^2(\mathbb{R})$ with respect to $\psi(x) \in L^2(\mathbb{R})$ is defined by

$$(Wf)(a,b) = \int_{-\infty}^{\infty} f(x)\psi^{a,b}(x)dx, \qquad (2.1)$$

where $a,b \in \mathbb{R}$, $a \neq 0$, and $\psi^{a,b}(x)$ is obtained from the function $\psi(x)$ by translating and dilating:

$$\psi^{a,b}(x) = |a|^{-1/2}\psi\left(\frac{x-b}{a}\right). \qquad (2.2)$$

This transform is useful when one wants to recognize or extract features of the function $f(x)$ from the transform domain.

2.2. 1D discrete wavelet transforms (DWTs). Suppose $\phi(x)$ and $\psi(x)$ are the scaling function and the corresponding wavelet, respectively, with finite support $[0,l]$, where l is a positive number. It is well known that $\phi(x)$ and $\psi(x)$ satisfy the following dilation equation:

$$\phi(x) = \sqrt{2}\sum_{s=0}^{l} h_s\phi(2x-s), \qquad (2.3)$$

$$\psi(x) = \sqrt{2}\sum_{s=0}^{l} g_s\phi(2x-s), \qquad (2.4)$$

where the h_s's and g_s's are constants called lowpass and highpass filter coefficients, respectively [8].

We will use the following standard notations:

$$\phi_{j,k} = 2^{j/2}\phi(2^j - k), \tag{2.5}$$

$$\psi_{j,k} = 2^{j/2}\phi(2^j - k). \tag{2.6}$$

Consider the subspace V_j of L^2 defined by

$$V_j = \text{Span}\{\phi_{j,k},\ k \in \mathbb{Z}\}, \tag{2.7}$$

and the subspace W_j of L^2 defined by

$$W_j = \text{Span}\{\psi_{j,k},\ k \in \mathbb{Z}\}, \tag{2.8}$$

where the subspaces V_j's, $-\infty < j < \infty$, form a multiresolution of L^2 with the subspace W_j being the difference between V_j and V_{j-1}. In fact, the L^2 space has an orthonormal decomposition as

$$L^2 = V_j \bigoplus \sum_{k=j}^{-\infty} W_k. \tag{2.9}$$

The projection of an L^2 function $f(x)$ onto the subspace V_j is defined by

$$f_j(x) = \sum_k \alpha_{j,k}\phi_{j,k}(x), \tag{2.10}$$

where

$$\alpha_{j,k} = \int f(x)\phi_{j,k}(x)dx. \tag{2.11}$$

Similarly, we can project $f(x)$ onto W_j by

$$w_j(x) = \sum_k \beta_{j,k}\phi_{j,k}(x), \tag{2.12}$$

where

$$\beta_{j,k} = \int f(x)\psi_{j,k}(x)dx. \tag{2.13}$$

Therefore, the function $f(x)$ can be decomposed by

$$f(x) = f_j(x) + \sum_{i=j}^{-\infty} w_i(x). \tag{2.14}$$

The projection $f_j(x)$ is called the *linear approximation* of the function $f(x)$ in the subspace V_j.

From (2.3)–(2.6), the projection coefficients $\alpha_{j,k}$ and $\beta_{j,k}$ of $f(x)$ in the subspaces V_j and W_j can be easily computed by the so-called *fast wavelet transform*:

$$\alpha_{j,i} = \sum_{s=0}^{l} h_s \alpha_{j+1,2i+s}, \qquad \beta_{j,i} = \sum_{s=0}^{l} g_s \alpha_{j+1,2i+s}. \tag{2.15}$$

Unlike in the continuous case where the wavelet transform is applied to the L^2 function $f(x)$, in the discrete case, we start by considering a set of discrete numbers which are the low-frequency coefficients of the L^2 function $f(x)$ at a fine-level subspace V_{j+1}.

In practice, DWTs are very useful. It is a tool that cuts up data, functions, or operators into different frequency components, and then studies each component with a resolution matched to its scale.

Assume that $\{h_k,\ k \in \mathbb{Z}\}$ and $\{g_k,\ k \in \mathbb{Z}\}$ are lowpass and highpass filter coefficients, respectively, which satisfy (2.3) and (2.4); then for a discrete signal $\{a_k,\ k \in \mathbb{Z}\}$, the low-frequency part $\{c_k,\ k \in \mathbb{Z}\}$ and the high-frequency part $\{d_k,\ k \in \mathbb{Z}\}$ of the DWT of $\{a_k\}$ are

$$c_k = \sum_{l} h_{l-2k} a_l, \qquad d_k = \sum_{l} g_{l-2k} a_l; \tag{2.16}$$

and the inverse DWT will give back $\{a_k\}$ from the knowledge of $\{c_k\}$ and $\{d_k\}$:

$$a_k = \sum_{l} \left(\tilde{h}_{k-2l} c_l + \tilde{g}_{k-2l} d_l \right), \tag{2.17}$$

where $\{\tilde{h}_k,\ k \in \mathbb{Z}\}$ and $\{\tilde{g}_k,\ k \in \mathbb{Z}\}$ are the reconstruction lowpass and highpass filter coefficients, respectively, and they can be obtained from the following equations:

$$g_k = (-1)^k \tilde{h}_{-k+1}, \qquad \tilde{g}_k = (-1)^k h_{-k+1}. \tag{2.18}$$

Based on the above fundamental backgrounds and some additional concepts, we will present several practical applications in the next section which will also indicate some advantages or disadvantages of different wavelet-based methods.

3. A case study

To examine statistics of signals and signal components is a very important task in studying the analysis of the well-known 1995 New Year's Day freak wave at the Draupner platform in the North Sea. In what follows, we will perform various wavelet analysis examinations on a given signal. We perform a multilevel wavelet decomposition, continuous wavelet transform with various wavelets, compression, denoising, as well as graphical examinational analysis of the corresponding wavelet coefficients which can be found in Figures 3.1, 3.2 3.3, 3.4, 3.5, 3.6, 3.7, 3.8, 3.9, 3.10, 3.11, 3.12, 3.13, 3.14, 3.15, 3.16, and 3.17. More precisely, we describe our studies of wavelet analysis for the given signal in more detail as follows.
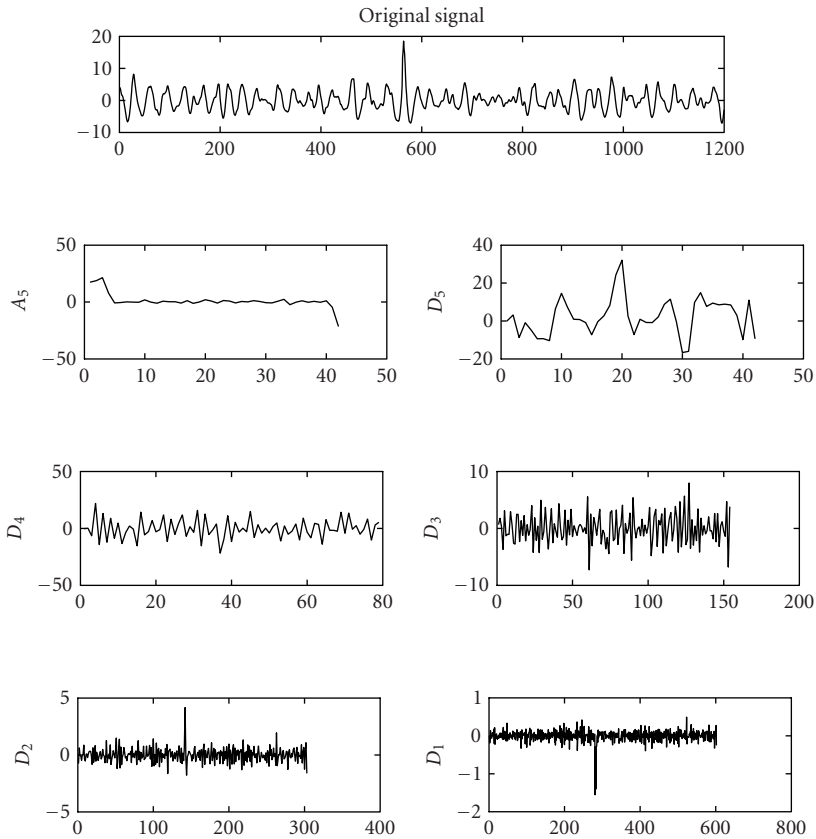
Figure 3.1. Decomposition of time series at level 5 with db3.

3.1. Multilevel decomposition.

A multiresolution decomposition of the signal is performed in Figures 3.1 and 3.2. As indicated in (2.9) and (2.14) and shown in those figures as well, the higher level is more coarser, while the lower level is more finer and close to the original signal. The higher-level approximation shows a more smoother version of the signal, while the lower-level decomposition is less smoother and has similar smoothness to the original signal. Multilevel decomposition in the details indicates different natures of the signal. Wavelet decomposition produces a family of hierarchical decompositions. The selection of a suitable level for the hierarchy usually depends on the signal and experience. At each level j, the j-level approximation A_j and a deviation signal called the j-level detail D_j are the decompositions of the lower-level approximation A_{j-1}. For example, in Figure 3.1, the signal is decomposed as $A_0 = A_1 + D_1 = A_2 + D_2 + D_1 = \cdots = A_5 + D_5 + D_4 + D_3 + D_2 + D_1$. Perhaps it is of most interest that the freak wave effect, the one single unusually high wave, only appeared at low scales D_1 and D_2. So the freak wave is basically a time localized event not affected by higher scales or low-frequency wave processes.
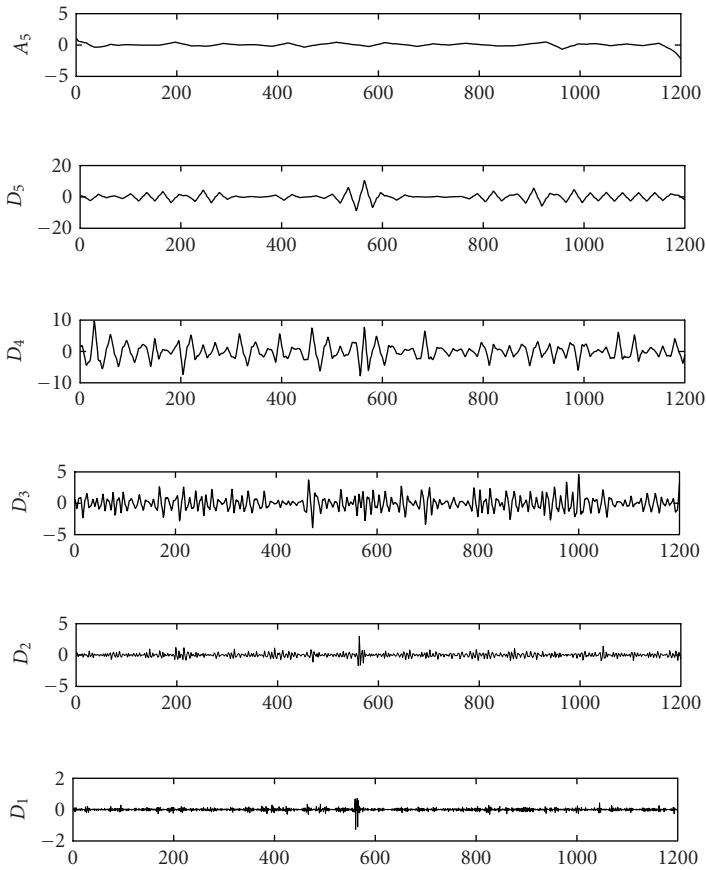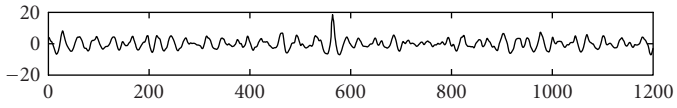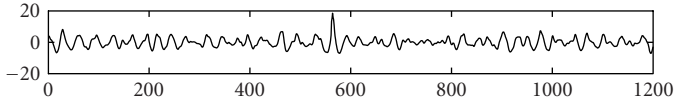
Figure 3.2. Approximation and details at level 5.

3.2. Compression. The compression of the signal is shown in Figure 3.4. Basically, the wavelet decomposition of the signal at level 5 is computed. For each level from 1 to 5, a threshold (0.3490) is selected and hard thresholding is applied to the detail coefficients as described in Section 2. The residual and reconstruction from compression are also shown in the figure. Essentially the idea of compression is that some small detail components can be thrown out without appreciably changing the signal. Only the significant components need to be transmitted, and significant data compression can be achieved. The way to choose small detail components depends on the threshold chosen for a particular application.

3.3. Reconstruction. Computation results of wavelet reconstruction at level 5 with db3 and the modified detail coefficients of levels from 1 to 5 are shown in Figures 3.2 and 3.3. The corresponding reconstruction and approximation are plotted in those figures. A reconstruction algorithm was used so that the compressed signal can be rebuilt in terms of the basic elements generated by certain a scaling function (Figure 3.4).
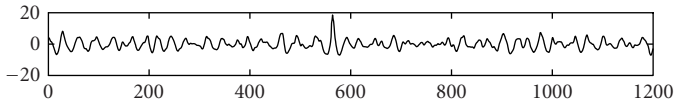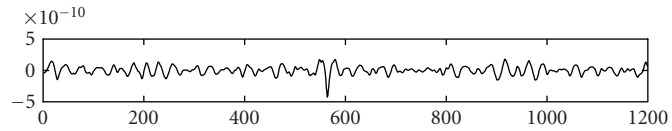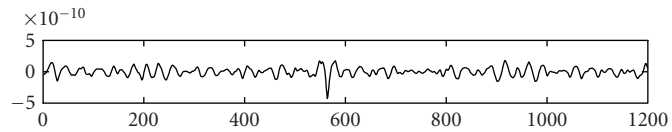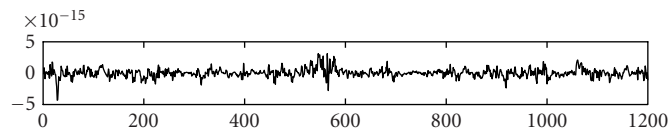
Figure 3.3. Reconstruction and approximation at level 5. (a) Original signal X. (b) A_0: reconstructed from the multilevel wavelet decomposition. (c) Sum of approximation and details: $A_5 + D_5 + D_4 + D_3 + D_2 + D_1$. (d) $X - A_0$. (e) X-Sum. (f) A_0-Sum.

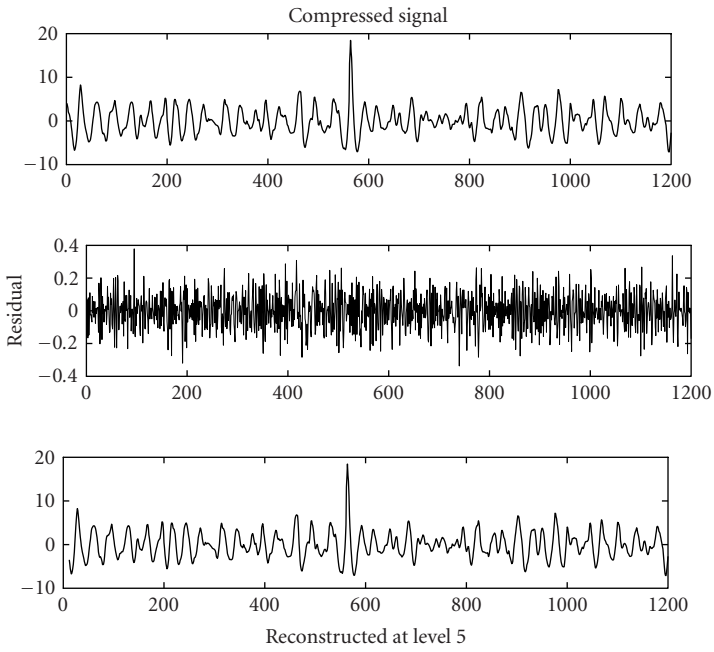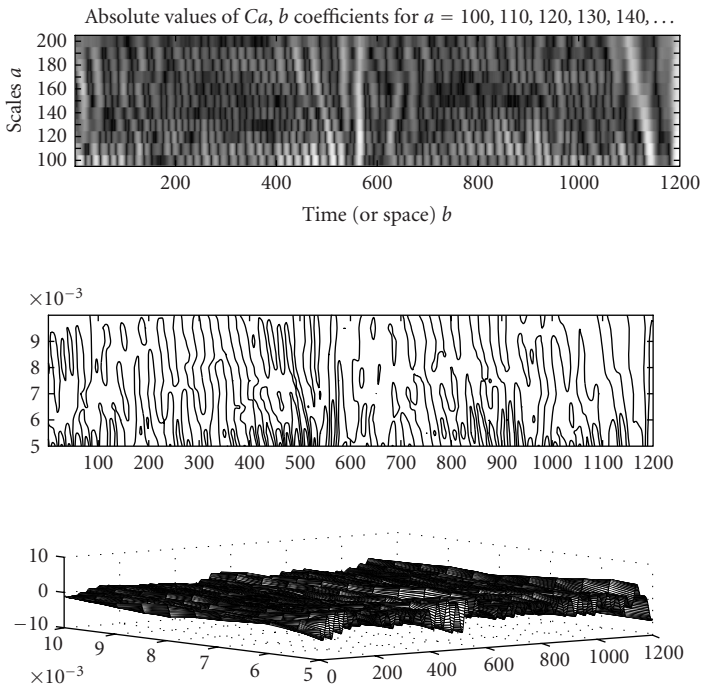Figure 3.4. Compression with global thresholding.
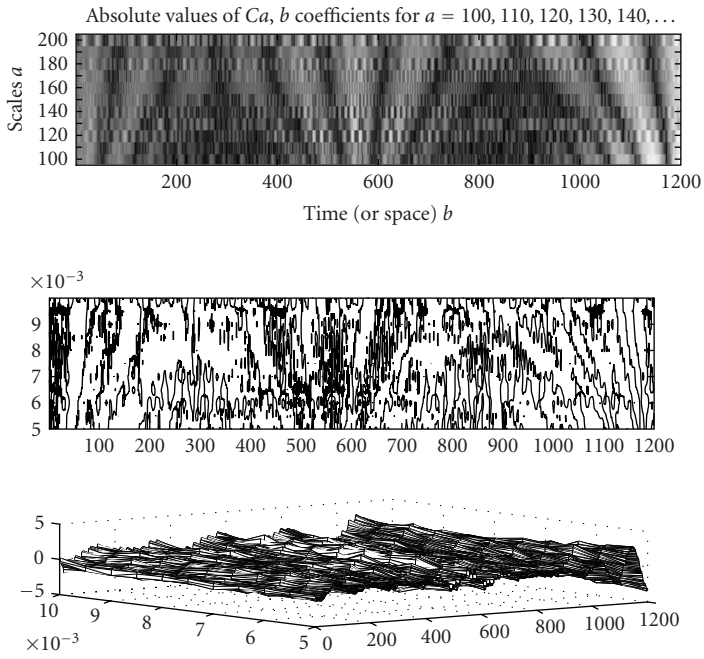

Figure 3.5. Continuous wavelet transform with db3.

Absolute values of Ca, b coefficients for $a = 100, 110, 120, 130, 140, \ldots$

Figure 3.6. Continuous wavelet transform with morlet wavelet.

Absolute values of Ca, b coefficients for $a = 100, 110, 120, 130, 140, \ldots$
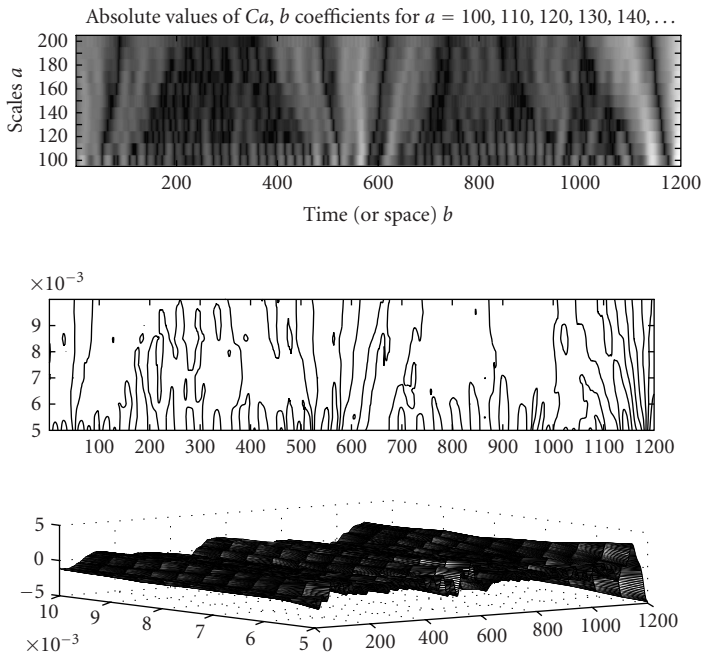
Figure 3.7. Continuous wavelet transform with Coiflet3.

Absolute values of Ca, b coefficients for $a = 100, 110, 120, 130, 140, \ldots$
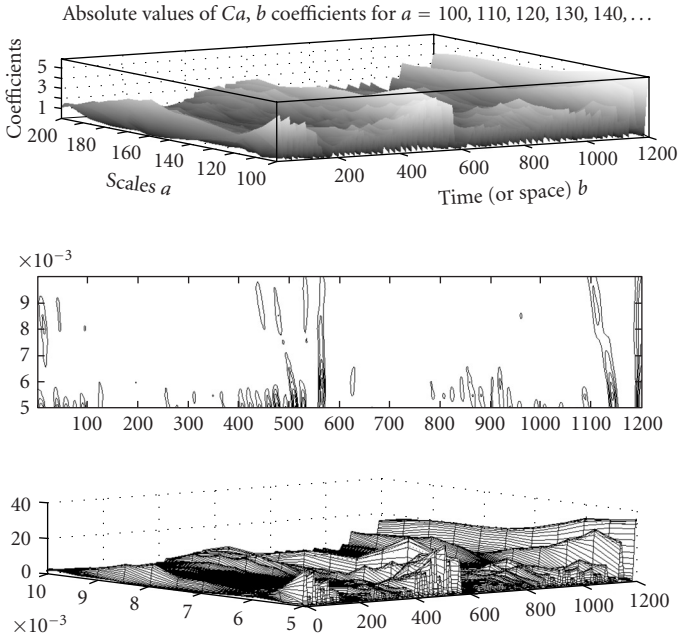
Figure 3.8. Wavelet spectrum with db3.

Absolute values of Ca, b coefficients for $a = 100, 110, 120, 130, 140, \ldots$
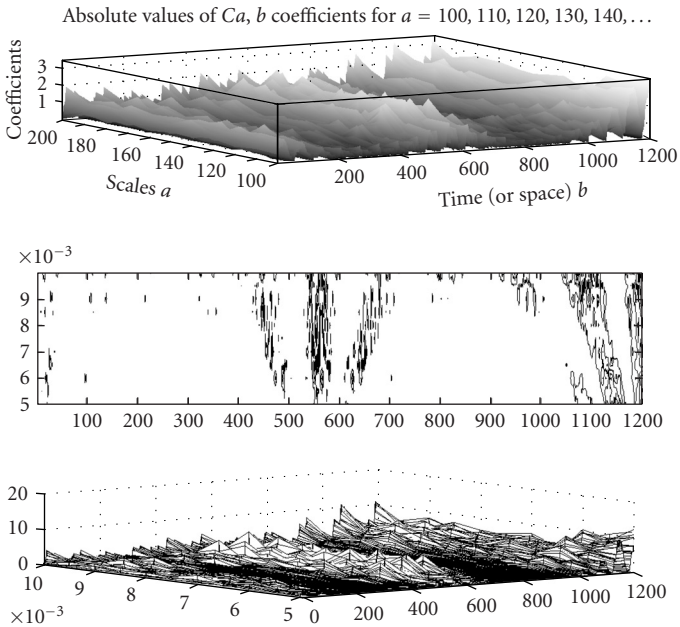
Figure 3.9. Wavelet spectrum with morlet.

Absolute values of Ca, b coefficients for $a = 100, 110, 120, 130, 140, \ldots$
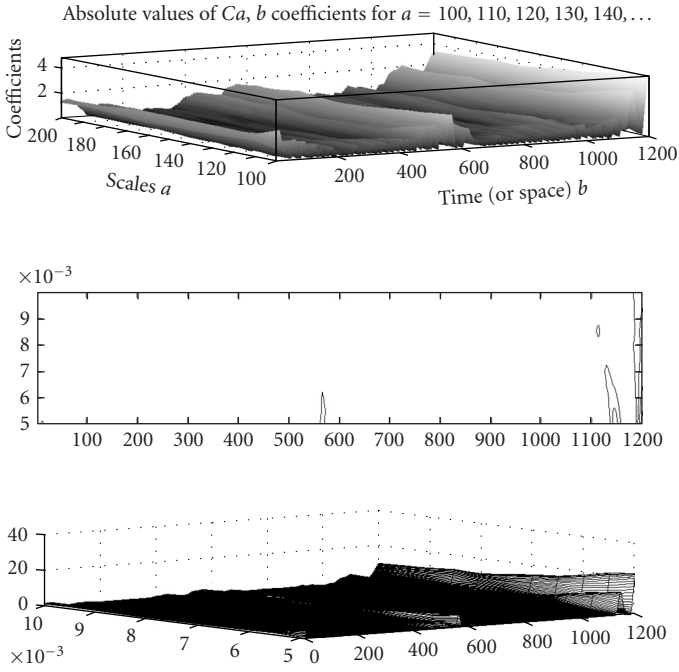
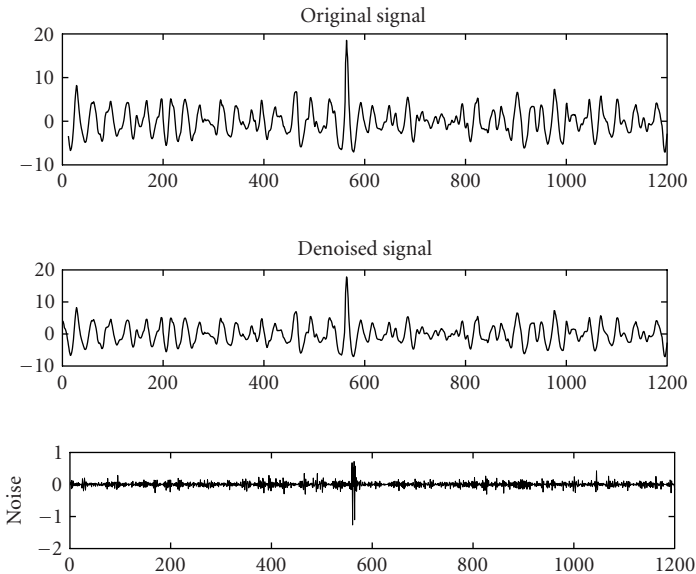Figure 3.10. Wavelet spectrum with Coiflet3.

Figure 3.11. Denoising thr. db3 with global thresholding. (Zero Coefficients: 50%, 2-norm reconstruction: 90.8868%.)
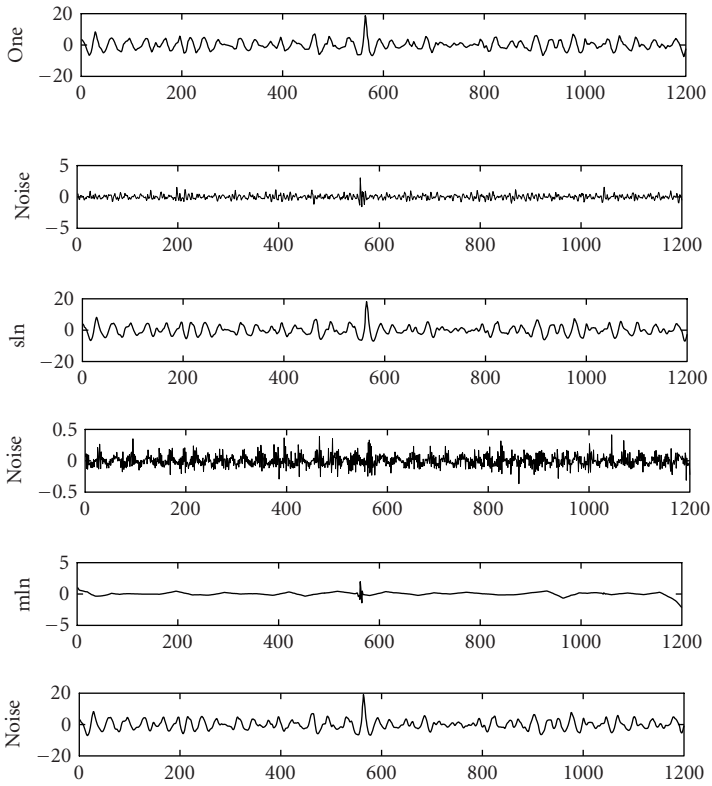
Figure 3.12. Denoised signal/basic /unscaled /nonwhite noise with db3.
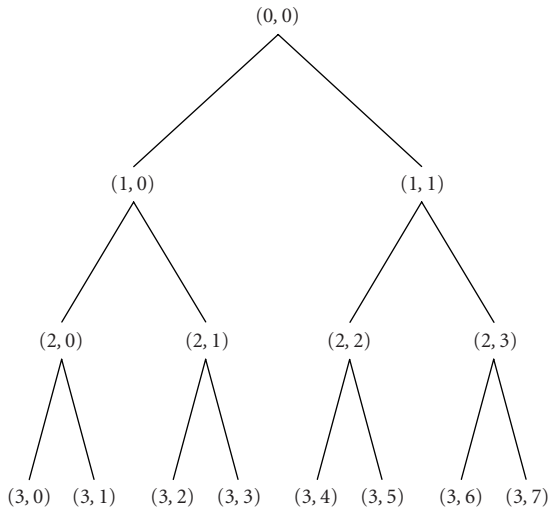
Figure 3.13. Best-level decomposition tree.
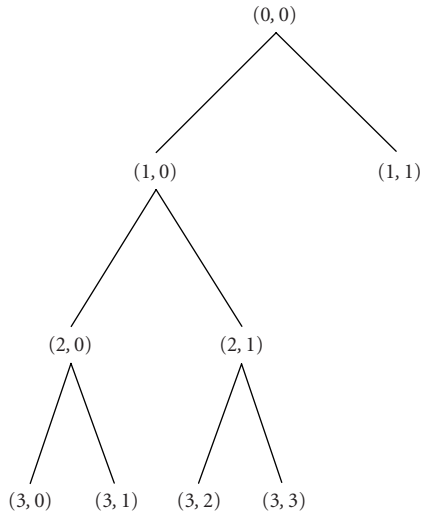
Figure 3.14. Wavelet packet with optimal subtree.
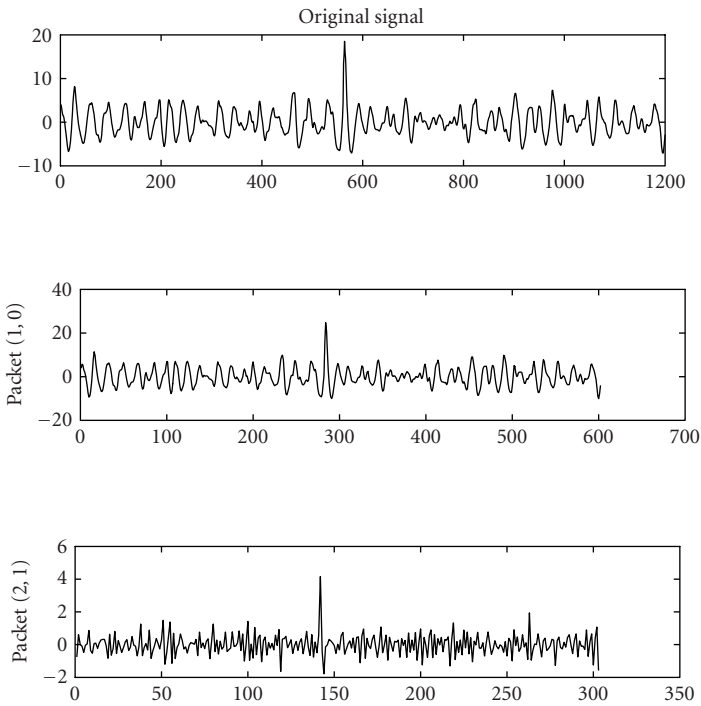
Figure 3.15. Wavelet packet with db3.

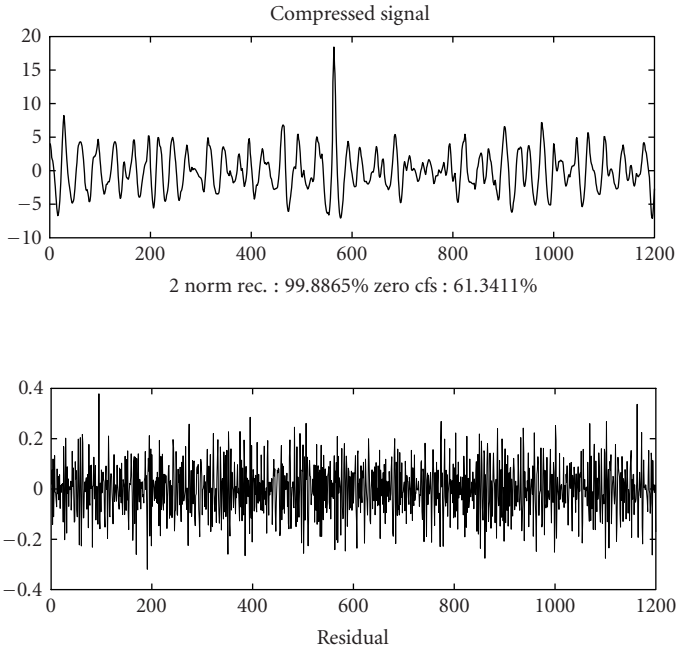Compressed signal

2 norm rec. : 99.8865% zero cfs : 61.3411%

Residual

Figure 3.16. Compression thr. wavelet packet with db3.

Denoised signal

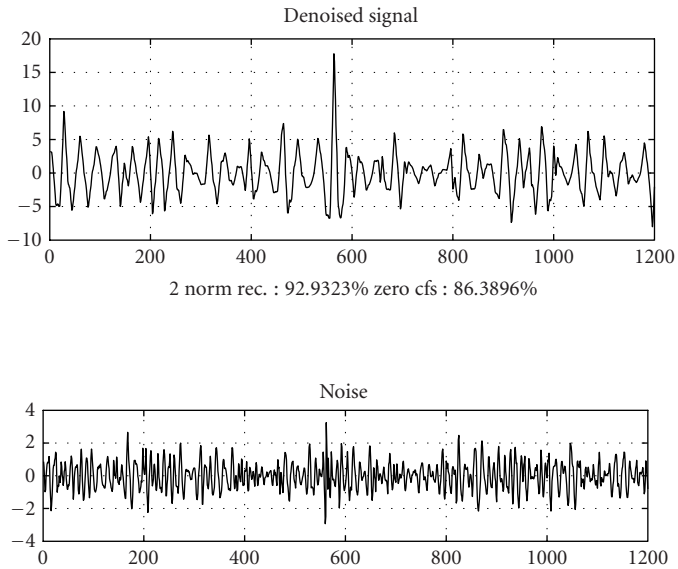2 norm rec. : 92.9323% zero cfs : 86.3896%

Noise

Figure 3.17. Denoising thr. wavelet packet with db3.

3.4. Wavelet coefficients. Performing continuous wavelet transforms, we obtain several results. Wavelet coefficients of analyzed signals with db3 are shown in Figure 3.5. The corresponding spectrum is shown in Figure 3.8. Wavelet coefficients of analyzed signals with Morlet wavelet are shown in Figure 3.6. The corresponding spectrum is shown in Figure 3.9. Wavelet coefficients of analyzed signals with Coiflet3 are shown in Figure 3.7. The corresponding spectrum is shown in Figure 3.10. The performances by using different wavelets can be viewed and compared while one searches for different natures and features of the corresponding wavelets. Again, the primary feature of freak waves is shown clearly at low scales in both discrete and continuous wavelet transform results. In Figures 3.5 to 3.10, Ca, b is defined as (2.1).

3.5. Denoising. The denoising results based on wavelet decomposition with different noise assumptions are shown in Figures 3.11 and 3.12. The denoised signal in Figure 3.11 is obtained by wavelet coefficient thresholding using global threshold 1.9482. The threshold used in Figure 3.12 is a mixture of Stein's unbiased risk estimate and the square root of the signal length. The three denoising methods used are general basic model (one), basic model with unscaled noise (sln), and basic model with nonwhite noise (mln). As one can see from the resulting signals, comparing with the original wave, it turned out that the method with unscaled noise is a better denoising method.

3.6. Wavelet packet. The wavelet packet method is a generalization of wavelet decomposition as shown above. Wavelet packet atoms are waveforms indexed by three parameters: position, scale, and frequency. For a given signal with respect to a given orthogonal wavelet, we generate a library of bases called wavelet packet bases. Each of these bases offers a particular way of coding signals, preserving global energy, and reconstructing exact features. We obtain numerous expansions of a given signal by using wavelet packets. We then select the most suitable decomposition of a given signal with respect to an entropy-based criterion. We analyze our signal into a decomposition tree with db3 as shown in Figure 3.13. We then select an optimal basis with the best level (Figure 3.14). The corresponding compression and denoising are shown in Figures 3.16 and 3.17, respectively. Some coefficients of subtrees are shown in Figure 3.15.

4. Concluding remarks

While this study is a first attempt in applying wavelet tools to exhaust various analyses on a set of freak wave data, it would be interesting to compare results for further studies on other waves or using different wavelets. It is also interesting to develop other studies by using interpolation methods [4] as well. Freak waves are a major threat to ships and offshore structures such as oil rigs, but they are difficult to predict. It seems that freak waves exist even in the ocean far away from strong current gradients. A wave must be at least 2.2 times the height of the largest 33% of the waves. Some freak waves are caused by strong currents or the chance reinforcement of two large waves, and a so-called "self-focusing" effect could also create outside waves [1]. The modeling of the waves from the point of view of the nonlinear Schrodinger equation was developed by several authors [1].

It would be interesting to construct a model and compare some simulations which will be compatible with the results derived from this paper.

References

[1]   K. B. Dysthe and K. Trulsen, *Note on breather type solutions of the NLS as model for freak waves*, Phys. Scripta **T82** (1999), 48–52.

[2]   H. M. Fritz and P. C. Liu, *An application of wavelet transform analysis to landslide-generated impulse waves*, Ocean Wave Measurement and Analysis (San Francisco, 2000) (B. L. Edge and J. M. Hemsley, eds.), American Society of Civil Engineering, Virginia, 2001, pp. 1477–1486.

[3]   P. A. E. M. Janssen, *Nonlinear four-wave interactions and freak waves*, J. Phys. Oceanogr. **33** (2003), no. 4, 863–884.

[4]   E.-B. Lin, *A survey on scaling function interpolation and approximation*, Applied Mathematics Reviews, Vol. 1, World Scientific, New Jersey, 2000, pp. 559–607.

[5]   P. C. Liu, *Wavelet spectrum analysis and ocean wind waves*, Wavelets in Geophysics (Maryland, 1993) (E. Foufoula-Georgiou and P. Kumar, eds.), Wavelet Anal. Appl., vol. 4, Academic Press, California, 1994, pp. 151–166.

[6]   ———, *Wavelet transform and new perspective on coastal and ocean engineering data analysis*, Advances in Coastal and Ocean Engineering Vol. 6 (P. Liu, ed.), World Scientific, 2000, pp. 57–101.

[7]   P. C. Liu and N. Mori, *Characterizing freak waves with wavelet transform analysis*, Rogue Waves 2000 (France) (M. Olagnon and G. A. Athanassoulis, eds.), Ifremer, France, 2001, pp. 151–156.

[8]   S. Mallat, *A Wavelet Tour of Signal Processing*, 2nd ed., Academic Press, California, 1999.

En-Bing Lin: Department of Mathematics, University of Toledo, Toledo, OH 43606, USA
E-mail address: elin@math.utoledo.edu

Paul C. Liu: Great Lakes Environmental Research Laboratory, National Oceanic and Atmospheric Administration (NOAA), Ann Arbor, MT 48105-2945, USA
E-mail address: paul.c.liu@noaa.gov

Special Issue on
Decision Support for Intermodal Transport

Call for Papers

Intermodal transport refers to the movement of goods in a single loading unit which uses successive various modes of transport (road, rail, water) without handling the goods during mode transfers. Intermodal transport has become an important policy issue, mainly because it is considered to be one of the means to lower the congestion caused by single-mode road transport and to be more environmentally friendly than the single-mode road transport. Both considerations have been followed by an increase in attention toward intermodal freight transportation research.

Various intermodal freight transport decision problems are in demand of mathematical models of supporting them. As the intermodal transport system is more complex than a single-mode system, this fact offers interesting and challenging opportunities to modelers in applied mathematics. This special issue aims to fill in some gaps in the research agenda of decision-making in intermodal transport.

The mathematical models may be of the optimization type or of the evaluation type to gain an insight in intermodal operations. The mathematical models aim to support decisions on the strategic, tactical, and operational levels. The decision-makers belong to the various players in the intermodal transport world, namely, drayage operators, terminal operators, network operators, or intermodal operators.

Topics of relevance to this type of decision-making both in time horizon as in terms of operators are:

- Intermodal terminal design
- Infrastructure network configuration
- Location of terminals
- Cooperation between drayage companies
- Allocation of shippers/receivers to a terminal
- Pricing strategies
- Capacity levels of equipment and labour
- Operational routines and lay-out structure
- Redistribution of load units, railcars, barges, and so forth
- Scheduling of trips or jobs
- Allocation of capacity to jobs
- Loading orders
- Selection of routing and service

Before submission authors should carefully read over the journal's Author Guidelines, which are located at http://www.hindawi.com/journals/jamds/guidelines.html. Prospective authors should submit an electronic copy of their complete manuscript through the journal Manuscript Tracking System at http://mts.hindawi.com/, according to the following timetable:

Manuscript Due	June 1, 2009
First Round of Reviews	September 1, 2009
Publication Date	December 1, 2009

Lead Guest Editor

Gerrit K. Janssens, Transportation Research Institute (IMOB), Hasselt University, Agoralaan, Building D, 3590 Diepenbeek (Hasselt), Belgium; Gerrit.Janssens@uhasselt.be

Guest Editor

Cathy Macharis, Department of Mathematics, Operational Research, Statistics and Information for Systems (MOSI), Transport and Logistics Research Group, Management School, Vrije Universiteit Brussel, Pleinlaan 2, 1050 Brussel, Belgium; Cathy.Macharis@vub.ac.be